Journal of Engineering Physics and Thermophysics, Vol. 73, No. 5, 2000

EXPERIMENTAL INVESTIGATION OF THE PROPAGATION OF HEAT WAVES OF ENERGY CONVERSION IN BLOWN-THROUGH POROUS MEDIA

G. A. Fateev, M. A. Silenkov, and Kyu-jong Kim

UDC 536:2:546.11

The method of metal-hydride energy conversion predicted earlier as a result of numerical modeling and realized in the regime of heat waves that propagate in porous media is confirmed experimentally. The metal-hydride thermal converter is made up of two channels filled with a porous medium. The thermal converting properties of porous media are governed by metal-hydride elements (thermal-converter poles) distributed along the length of the channels. The elements of each channel contain zirconium-based alloys that are capable of rapidly and reversibly interacting with hydrogen with the formation of hydrides. The effect of the intensification of a cold wave (in a channel with low-temperature poles) is confirmed experimentally. Its amplitude attains the maximum low temperature that is permissible for a metal-hydride pair and exceeds the adiabatic temperature of the hydrogenation reaction in the channel of the thermal converter.

The method of metal-hydride conversion of heat energy is based on the property of some alloys M to rapidly and reversibly interact with hydrogen with the formation of a hydride [1]:

$$M + \frac{n}{2} H_2 = MH_n \pm \Delta h \,. \tag{1}$$

The transition of hydrogen from the free state to hydride phases of alloy is accompanied by the transfer of heat and mass in the hydride layer under the conditions of a rapidly establishing equilibrium between the components of reaction (1) [2].

In the traditional method, use is made of alloys that exchange hydrogen [3] (metal-hydride pair). The alloys in the pair are dissimilar in their properties (are polar in relation to each other). Accordingly, the vessels that contain alloys and are united into a single energy-converting element will be called in what follows thermal-converter poles. The interaction with hydrogen at the same pressure is governed by a different temperature (Fig. 1). The character of the relationship between the temperature and the pressure is typical of the saturation line of an equilibrium phase transition, for example, in a water–vapor system. The phase transition of hydrogen to a hydride form in the alloy with a greater hydrogen affinity is characterized by a higher temperature than in the alloy with a lower affinity. This alloy in the pair and the pole that corresponds to it will be called high-temperature (HT), and the other will be referred to as low-temperature (LT).

The cycle of heat-energy conversion involves two stages (Fig. 1). In the first stage, the metal-hydride pair is activated (the charging stage). For this purpose, the high-temperature pole is heated from the heat source with a temperature T_{Hd} and the hydrogen is compulsorily transferred from it to a low-temperature pole. The sorption heat of the low-temperature pole is, accordingly, removed from it to the ambient medium (T_0). In the second stage, the charged pair operates as a thermocompressor (heat pump) (the discharging stage). The hydrogen returns spontaneously from the low-temperature pole to the high-temperature one, transferring efficiently the heat from the zone of phase transfer with a temperature T_{hLd} to the zone of phase transfer with a higher

Academic Scientific Complex "A. V. Luikov Heat and Mass Transfer Institute," National Academy of Sciences of Belarus, Minsk, Belarus. Translated from Inzhenerno-Fizicheskii Zhurnal, Vol. 73, No. 5, pp. 1093-1108, September–October, 2000. Original article submitted June 2, 2000.

1062-0125/00/7305-1069$25.00

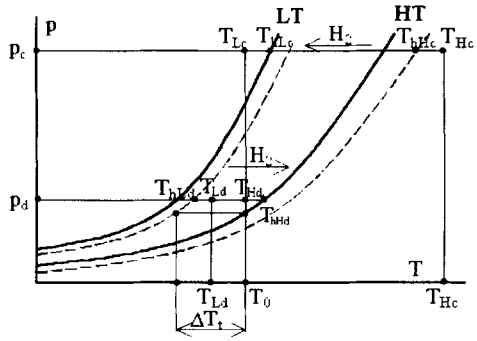

Fig. 1. Diagram illustrating the Van't Hoff equilibrium for a hydride pair: the solid curves show the equilibrium in hydrogen sorption; the dashed curves, in desorption.

temperature T_{hHd}. More detailed information on the realization of traditional metallohydride cycles of heat-energy conversion in all their variants can be obtained in [3].

The main advantages of the cycle of metal-hydride conversion of heat energy are governed by the rapid and reversible reaction of hydride formation that is realized in a wide temperature range (from hundreds of degrees above 0°C to −120°C [4]), the high heat of reaction, and the possibility of modifying the alloy by adapting it to specific conditions of the process. Modification of the alloy means a change in the position of the curves (Fig. 1) relative to the temperatures of heat tanks T_{Hc} and T_0 that initiate the process and the required temperature of heat conversion T_{Ld}. One of the main characteristics of the conversion of heat energy is the temperature and the heating (refrigerating) capacity. It follows from Fig. 1 that the maximum high thermal effect ΔT_t is attained in the case of the thermal equilibrium between the temperatures of the heat tanks (of the ambient medium T_0 and the refrigerator) and the temperatures of the phase transitions inside the thermal-converter poles that are in contact with these tanks. Assuming that the phase-equilibrium curves (see Fig. 1) are the Van't Hoff curves

$$p = p_0 \exp\left(\frac{\Delta S}{T} - \frac{\Delta h}{RT}\right), \tag{2}$$

we represent the expression for the limiting temperature of heat conversion that is attained in a low-temperature hydride (LT) paired with a high-temperature one (HT) in the form

$$T_{hLd} = \frac{\Delta h_L}{\Delta S_L - \Delta S_H + \dfrac{\Delta h_H}{T_0}}. \tag{3}$$

The actual heat transfer is realized in the presence of a finite difference of the temperatures between the phase transitions at the poles T_{hHd} and T_{hLd} and the heat tanks or their heat-transfer agents T_{Hd} and T_{Ld}. Accordingly, the equilibrium thermal effect of the refrigeration cycle will be determined as

$$\Delta T_{t\,max} = T_{hLd} - T_{Ld}.$$

In what follows, the quantity $\Delta T_{t\,max}$ will be called the thermal limit of heat-energy conversion. The actual thermal effect will be

$$\Delta T_t = T_{Ld} - T_{Hd}.$$

The main drawbacks of the traditional method of heat conversion are associated with the features of the phase equilibrium in the hydride pair and with nonequilibrium effects of heat exchange in cyclic realization of the process.

In Fig. 1, equilibrium properties of each hydride (both low-temperature and high-temperature) are presented by a pair of curves that reflect the hysteresis of equilibrium, namely, an equilibrium pressure in sorption higher that the equilibrium pressure in desorption. The temperatures of the heat tanks that exchange heat via the metal-hydride thermocompressor are coordinated around the equilibrium curves so that the thermal efficiency of the process is lost in the stage of both charging and discharging. In particular, $\Delta T_{t\,max}$ turns out to be smaller than it would be in the absence of hysteresis (for example, if the equilibrium were presented only by solid curves or only by dashed curves). Another feature of the equilibrium that also leads to a reduction in the thermal efficiency of the process and is associated with the dependence of equilibrium pressure on concentration will be considered below in a more detailed analysis of the equilibrium.

The nonequilibrium of the process that is governed by the difference between the heat-tank temperature and the phase transition temperature leads in a direct manner to the loss of the thermal efficiency of the process. As was shown above, $\Delta T_{t\,max}$ exceeds ΔT_t in absolute value (Fig. 1). The obvious strategy of bringing heat-exchange conditions closer to equilibrium at which the heat exchange would be realized for the minimum temperature difference requires a reduction in the thermal load or thermal resistance between the heat tank and the zone of phase transition of the hydrogen inside the hydride mass:

$$T_{hLd} - T_{Ld} = (R_{tL\,in} + R_{tL\,ex})\, W_L .$$

One of the problems of hydride heat conversion is the high internal thermal resistance between the pole surface and the zone of phase transition of hydrogen that cuts deeper into the alloy as it is saturated with hydrogen. In interacting with the hydrogen the alloy develops a finely divided structure with a low thermal conductivity (of about 1 W/m^2). An increase in the thermal conductivity (the decrease in $R_{tL\,in}$) is attained by creating a cross-linked hydride mass with the use of supplementary additions of a highly heat-conducting material [5]. The reduction in the external thermal resistance $R_{tL\,ex}$ is ensured by the development of the surface of external heat exchange, for example, by finning the exterior surface of the pole. Thus, technical measures that are aimed at reducing the nonequilibrium of heat exchange lead to an increase in the mass capacity and total heat capacity of the pole.

Irreversible heat losses due to the cyclic realization of the process are an additional problem of hydride heat conversion. The alternating phase transition is accompanied by the release or absorption of heat, while each pole is alternately switched between the media (heat tanks) involved in the process. Therefore at the beginning of the discharging stage the entire mass of the pole has a temperature not lower than the ambient temperature, and it is required that part of the phase-transition energy be expended before the pole is capable of receiving heat from a cold tank. This part of the energy is irreversibly lost. Thus, the useful heat employed in the refrigeration cycle is equal to

$$Q_L = -\Delta h_L + m_{hL}\, c_{hL}\, (T_0 - T_{Ld}) + m_{pL}\, c_{pL}\, (T_0 - T_{Ld}) .$$

Its magnitude decreases as the mass capacity of the hydride or the pole increases. Therefore, improvement of the energy characteristics of the process will naturally lead to a reduction in its thermal efficiency. As a result, the thermal capabilities of the hydride conversion of heat energy which are realized in practice are limited by the temperatures of a refrigeration cycle that is acceptable only for conditioning purposes, and there are extremely limited data on a refrigeration cycle with a temperature below 0°C [1, 6].

An alternative method of metal-hydride heat conversion is called upon to overcome the basic problems of the traditional method that consist of the presence of irreversible heat losses in an unsteady cyclic realization of the process. This, in particular, occurs at the beginning of the discharging stage, where part of the free energy of a nonequilibrium pair is expended on imparting the required temperature to the pole (precooling to the working temperature of the refrigeration cycle).

The main idea of the new method is the employment of the transfer properties of a porous medium that make it possible to transport the heat (cold) from the pole that exhausted its service life and comes out of either stage of heat conversion to the pole that comes into this stage [7]. With this organization of the process

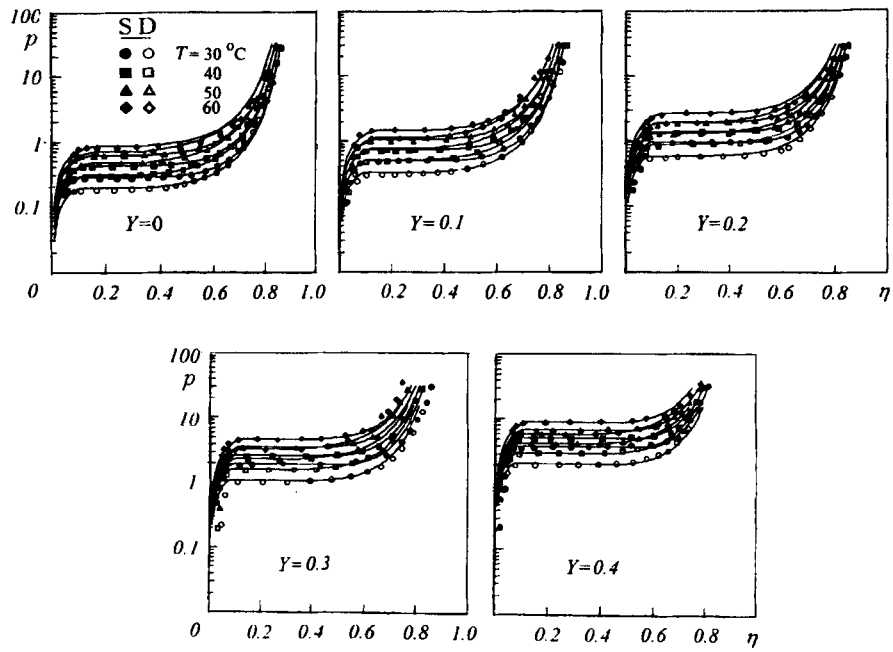

Fig. 2. Equilibrium isotherms for $Zr_{0.9}Ti_{0.1}Cr_{1-Y}Fe_{1+Y}H_n$. The dots are the experiment; the curves are the optimization by formula (5). p, atm.

the converted heat is accumulated in the heat wave rather than in the flow of the heat-transfer agent. This enables one to abandon the use of a low mass-intensive hydride procedure. The employment of a heat-intensive porous medium leads in a natural manner to a decrease in the adiabatic temperature of the system; this temperature is the limit of the thermal efficiency of the process with a uniform distribution of the phase-transition energy over all the elements of the structure (i = 1 ... N) that are involved in the heat conversion:

$$T_{ad} = \frac{\Delta m_{H_2} \Delta h}{\sum_{i=1}^{N} m_i c_i} + T_0 . \tag{4}$$

The special properties of the transfer in a porous medium enable one to overcome the adiabatic limit (4) and to bring the process closer to its equilibrium thermal limit, which is governed by the nature of the metal-hydride pair (3).

1. Properties of Hydride-Forming Alloys. In the experimental investigation, use was made of zirconium-based, hydride-forming alloys that were developed and tested at the Korean Institute of Science and Technology (KAIST) at the department headed by Prof. J.-Y. Lee [8, 9]. The alloys are determined by the structural formula AB_5^2 (the Laves family of alloys). The alloys' chemical composition corresponds to the generalized formula $Zr_{0.9}Ti_{0.1}Cr_{1-Y}Fe_{1+Y}$, where Y can vary from 0 to 0.4.

Figure 2 presents the results of measuring the equilibrium properties of some specimens of the indicated family of alloys $Zr_{0.9}Ti_{0.1}Cr_{1-Y}Fe_{1+Y}$. The dependence of equilibrium pressure on concentration is determined by the equilibrium area within whose limits the pressure changes insignificantly. This indicates a complex structure of the phase composition of the hydride. The Van't Hoff curves shown in Fig. 1 represent a correlation of the pressure referred to the middle of the area (see Fig. 2) based on the temperature of the isotherms.

The use of alloys whose properties can be changed through the selection of their composition makes it possible to freely adapt the alloy pair to the thermal conditions of heat-energy conversion. To charge a rigid hydride pair with a great difference in Y, it is necessary to use a high-temperature heat source. On the contrary,

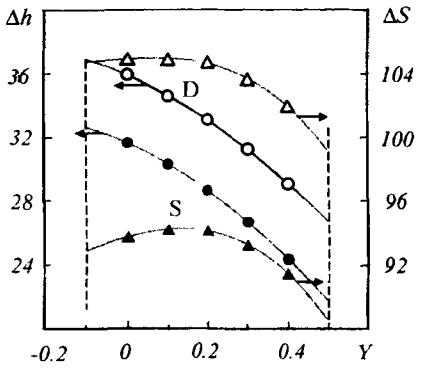

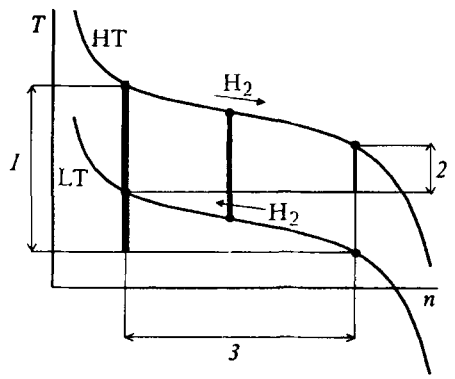

Fig. 3. Generalization of experimental data on the equilibrium in hydride systems based on $Zr_{0.9}Ti_{0.1}Cr_{1-Y}Fe_{1+Y}$ alloys. Δh, kJ/mol; ΔS, J/(mol·K).

Fig. 4. Dynamics of the thermal effect of a pair in the discharging stage: 1) starting thermal limit of the pair; 2) final limit; 3) concentration range.

during the conversion of low-potential heat it is necessary to create a soft pair characterized by close values of Y for the used hydrides. Since electric energy is used as a source initiating heat-energy conversion in the proposed series of tests, we selected a maximum rigid pair for the given alloy family, namely, $Zr_{0.9}Ti_{0.1}CrFe$ (Y = 0) as a high-temperature alloy and $Zr_{0.9}Ti_{0.1}Cr_{0.6}Fe_{1.4}$ (Y = 0.4) as a low-temperature one.

For a detailed description of the hydride's equilibrium condition the de Boer equation was used [10]:

$$p = p_e \frac{F(T,\eta)}{F(T,1/3)}, \quad p_e = p_0 \exp\left(\frac{\Delta S}{R} - \frac{\Delta h}{RT}\right),$$
$$F(T,\eta) = \frac{\eta}{1-\eta}\exp\left(\frac{\eta}{1-\eta} - \frac{k_T\eta}{T}\right), \quad \eta = \frac{n}{n_{max}}. \tag{5}$$

Figure 3 shows how the Van't Hoff constants Δh and ΔS obtained as a result of the optimization of experimental data for each Y (Fig. 2) depend on the alloy's composition. The generalization of the equilibrium properties of hydrides in the parameters of the de Boer equilibrium (5) has the following form:

$$\Delta h_S = 31.63 - 11.79Y - 16.02Y^2,$$
$$\Delta S_S = 93.78 + 6.948Y - 19.70Y^2 - 30.67Y^3,$$
$$k_{T1S} = 8 + 1.5Y, \quad k_{T2S} = 6.6 + 3.0Y, \quad n_{maxS} = 3.5,$$
$$\Delta h_D = 35.91 - 11.39Y - 14.27Y^2,$$
$$\Delta S_D = 104.9 + 1.401Y - 5.913Y^2 - 40.50Y^3, \tag{6}$$
$$k_{T1D} = 8 + 2.5Y, \quad k_{T1D} = 6 + 2.5Y, \quad n_{maxD} = 3.5.$$

The coefficients k_{T1} and k_{T2} characterize the slope of areas on the equilibrium isotherms (see Fig. 2). The coefficient k_{T1} is determined for the range of concentrations η from 0 to 1/3, while k_{T2} is determined for η from 1/3 to 1.

Equations (6) give exhaustive information about any alloy of the family, including, too, the assumed extrapolation of the properties beyond the investigated range (Fig. 2).

The dependence of equilibrium pressure on concentration determines yet another feature of heat and mass exchange that consists of the dynamics of the thermal effect of the metal-hydride pair as the hydrogen is

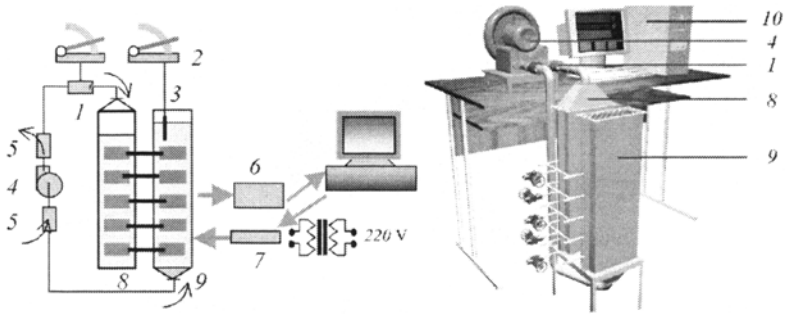

Fig. 5. Schematic diagram and a three-dimensional representation of an experimental setup: 1) Venturi tube; 2) micromanometers; 3) static-pressure tube; 4) pump; 5) controllers of the air flow rate; 6) commutator of thermocouples and analog-to-digital converter; 7) thyristor block; 8) high-temperature channel; 9) low-temperature channel; 10) system of data collection and processing.

redistributed in its poles. The illustration of this feature is executed on the basis of the consideration of the equilibrium isobars that can be reproduced from Eqs. (5) in the parameters (6) and is presented in Fig. 4. As follows from this figure, the maximum value of the thermal effect of the heat-energy conversion relates to the beginning of the discharging stage. It is exactly this high-potential part of energy in traditional technology that is irreversibly lost in the initial stage for pre-cooling the pole to the temperature of the cold tank. Then the thermal effect decreases as the pair's concentration resource is exhausted. In the case of a significant decrease in the thermal effect, the continuation of the process loses its meaning because of the decrease in its efficiency or a beyond-limit relationship between temperatures ($T_{Ld} - T_{hLd} < 0$, see Fig. 1), at which the process becomes energy-unprofitable. The indicated limitation is so substantial that in traditional technology use is made of only about half of the hydrogen capacity of the hydride [11]. This fact finds confirmation on the basis of a numerical analysis of the process using real-equilibrium dependences (5) and (6) [12].

2. Experimental Setup and the Method of Experimental Investigation. The schematic diagram of the experimental setup that realizes an alternative method is presented in Fig. 5. Its main component is a two-channel thermal converter. The channels are filled with porous media. The thermal converters' poles are built into the media. The channels are provided with devices to pump through them flows of air with assigned flow rates, as well as with devices for control of the air flow rate. Each of the metal-hydride-pair poles located in the high-temperature channel contains an independent electric heater. The power of the heaters is set using a transformer. The operation of the heaters is controlled by a block of thyristors. The temperature field in the channels of the thermal converters is recorded using a set of thermocouples that are distributed inside the hydride layer, on the surfaces of the poles, on the pole fins, and in the porous medium. The recording of the thermocouples' readings and the control of the operation of the heaters by switching them on and off is carried out with the help of a computer by a specially developed program. The indicated configuration of the experimental setup allows a rather flexible control of the operation of the thermal converters aimed at seeking the optimum characteristics of the process. At the same time, arbitrary distribution is allowed of the established power of the heaters in the sequence of the poles and arbitrary control of the power of each heater.

To realize the alternative method the following procedure was used. In the first stage of the process when the setup was in the starting condition determined by the ambient temperature in all its elements heating of all the poles of the high-temperature channel to the established temperature was carried out. Then blowing of the low-temperature channel was started to remove the heat released during the hydrogen sorption in the poles located in this channel and, consequently, to ensure a rather deep initial charging of each pair. The propagation of heat waves in a system thus prepared was controlled by assigning velocities to the air flows in each channel.

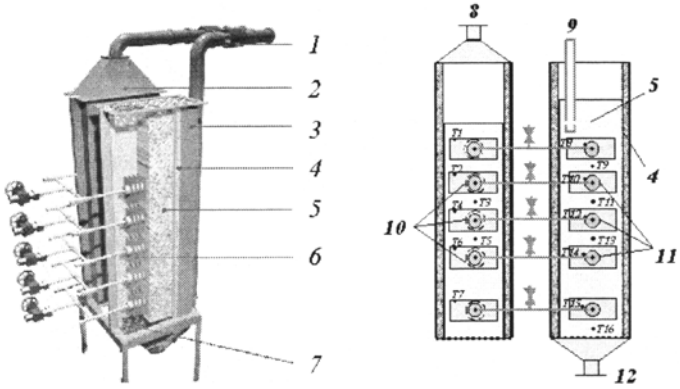

Fig. 6. Schematic diagram and a three-dimensional representation of thermal-converter channels: 1) Venturi tube; 2) high-temperature channel; 3) low-temperature channel; 4) heat insulation; 5) porous medium; 6) metal-hydride pair; 7) metal screen; 8) air-injection pipe; 9) static-pressure tube; 10) electric heaters; 11) metal-hydride poles; 12) air-suction pipe.

The schematic diagram of a *two-channel thermal converter* is given in Fig. 6. Each channel of the thermal converter represents a steel box with heat-insulated interior surfaces. The high-temperature channel is insulated with layers of sheet asbestos glued on its interior surface. The low-temperature channel is insulated with a single 1-cm thick layer of foam plastic. The free internal cross section of each channel is 60 × 160 mm^2, while its height is 488 mm.

The high-temperature channel in the upper part has a funnel for pumping the air flow through it from top to bottom. A similar funnel is installed in the lower part of the low-temperature channel (Fig. 6) for drawing the air flow through this channel in the same direction (from top to bottom) to create codirected heat waves in the two channels.

The finned poles of the thermal converters were located in such a way as to cover as fully as possible the cross section of the channel. This was facilitated by the selection of the overall dimensions of the poles. The length of the copper tube of the pole which contains the metal hydride is 150 mm. The transverse size of the pole was determined by a width of the fins of 50 mm. The height of the fins was 35 mm. The reduced size of the fin's height (compared to its width) was due to the general concept of the transfer of heat waves in a porous medium. According to this concept, the conditions for an optimum process are obtained at a maximum high quality of thermal contact between the phase-transition zone inside the pole and the porous medium adjacent to the pole and at a minimum thermal conductivity of the porous medium in the direction of gas flow. Both conditions turn out to be in a certain contradiction, whose partial solution is obtained by the selection of a fin with a reduced size in the direction of the propagation of heat waves.

The poles of the thermal converters were distributed in such a way that the distance between them was 10 mm. The same distance is preserved between the lower poles and the grids that limit the channels in their lower part. The upper part of the internal space of the channels was left for a possible variation of the location of the poles aimed at a later study of the influence of the distance between them on the efficiency of the process.

The internal space of the channel was filled with a porous medium, which in this case represented a *layer of dispersed material* loosely poured into each channel.

In solving the problem of distributing the thermocouples inside the channels of the thermal converter our goal was to obtain the maximum information on the dynamics of the temperature field in the propagation of the heat wave in the channels of the thermal converter, as well as on the thermal resistance inside the pole and the quality of thermal contact of the pole's exterior surface with the porous medium. To do this the thermocouples were placed both inside each pole and on their surfaces, and also in the porous medium between

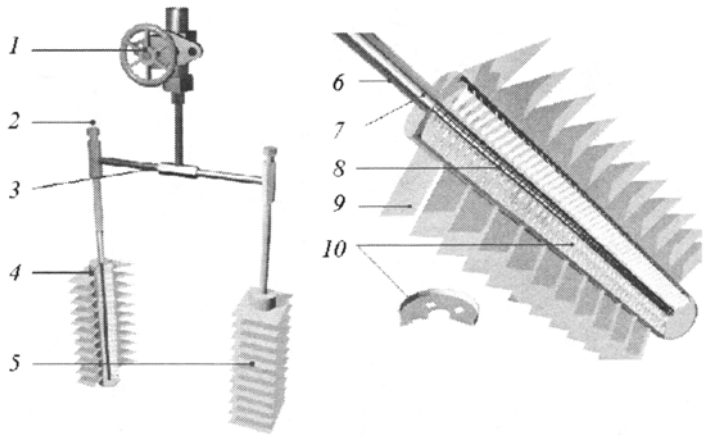

Fig. 7. Three-dimensional representation of a metal-hydride pair and an individual pole: 1) hydrogen valve; 2) thermocouple lead; 3) hydrogen channel; 4) high-temperature pole; 5) low-temperature pole; 6) channel for hydrogen transport; 7) thermocouple; 8) hydrogen artery; 9) external fin; 10) internal fin.

the poles. The location of the thermocouples and their numbers adopted during the description of the experimental results are shown in Fig. 6.

The two poles that represent independent vessels containing heterogeneous hydride-forming alloys, for example, selected from the Laves alloy family (see item 1), charged with hydrogen, and connected by a channel for free exchange of hydrogen between the poles, are a *metal-hydride pair* (Fig. 7). In the laboratory experiment, copper tubes 150 mm in length, 20 mm in diameter, and with 0.5 mm-thick walls were used as vessels. The poles contain internal 100 μm-thick copper-foil fins distributed with a 3-mm step and an internal artery for the transport of hydrogen along the pole over its axis that represents a tube rolled from a steel net. The free internal space of the pole between the interior surface and the artery is filled with an alloy. The mass of the alloy in each pole is 135 g.

Copper fins were soldered on the exterior surface of the poles. The thickness of the fins of the high-temperature pole was 0.35 mm, and that of the low-temperature one was 0.15 mm. The step between the fins was 12 mm.

Coiled around the high-temperature poles were electric heaters from Nichrome wire in ceramic insulation. Each pole of the pair was provided with a Chromel–Alumel thermocouple soldered into a stainless-steel case and hermetically installed inside the hydrogen artery.

The metal-hydride pairs contained valves for charging them with hydrogen; the values were located in the form of extensions on copper capillaries (4 mm) that connected the poles of the pairs.

The charging of the metal-hydride pair with hydrogen and the subsequent activation of the alloys seek to saturate them with hydrogen and to convert them into a hydride form. The amount of hydrogen introduced into the metal-hydride pair is a parameter that optimizes the metal-hydride cycle in its thermal and energy characteristics. The optimum amount of hydrogen is established experimentally or by means of numerical analysis.

A series of intermediate saturations of the alloys with hydrogen with the subsequent removal of it for their initial activation was performed on a hydrogen stand. Initially, the alloy was exposed to vacuum for a long time (up to 10 h) with a simultaneous heating of the poles to 300°C. Then the hydrogen was threefold supplied to the pair and was subsequently removed to the vacuum. The metal-hydride pair was cooled in supplying the hydrogen and was heated in the thermostat volume in removal.

The final charging was carried out into the pair that was completely emptied of hydrogen by heating and evacuation. We measured out the hydrogen reckoning that the hydride of the high-temperature pole that had absorbed all the hydrogen would correspond to the stoichiometric relation $Zr_{0.9}T_{0.1}CrFeH_2$. Since the mo-

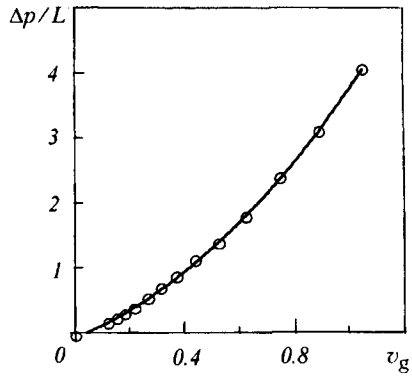

Fig. 8. Approximation of the data of calibration of a static-pressure tube. $\Delta p/L$, kPa/m; v_g, m/sec.

lecular weight of the high-temperature alloy is equal to 194.7 g/mol about 16 liters of hydrogen are required to charge 135 g (0.693 mol) of this alloy to the indicated stoichiometrtic composition. The prepared metal-hydride pairs (activated and charged by hydrogen) were installed into the thermal-converter channels, following which the channels were filled with a porous medium.

We used an aggloporite layer as the *porous medium*. Prior to its use, the aggloporite was crushed and was screened. A 0–5-mm fraction was used for filling the channels. The density of the layer measured by an independent method was 1200 kg/m^3. The heat capacity and thermal conductivity of the aggloporite layer are estimated to be 790 J/kg and 0.3 W/(m·K).

3. Means of Controlling and Measuring Gas Flows. One parameter that governs the thermal-conversion power and the thermal efficiency of the process in the regime of heat waves is the velocity relation of the gas flows in the channels of the device (see Fig. 5). A VP400/08-type peripheral pump was used as the propeller for the air flow. The pump capacity is 0.8 m^3/min with a head of 400 millimeters of water column. The vortex principle of operation corresponds to a tendency for retaining the capacity with increase in the hydraulic resistance of the gas channel. A drawback of the pump of the indicated type is its low efficiency, as a result of which the air flow pumped at the ambient temperature was heated by 15–20°C. The obvious advantage of the pump is its hermetic version. This made it possible to supply both channels with independent air flows using only one pump (Fig. 5). To independently control the air flows in the channels for the indicated circuit of connecting them to the gas main, we used gate-valve controllers. For this purpose, several holes were milled along the generatrix of the tube; the holes were covered by a coupling to change the cross section for the flow of air discharged from the tube on the discharge line or the air sucked into the tube on the suction line.

To measure the flow rate on the discharge line (the high-temperature channel, Fig. 5), we manufactured a Venturi tube. The configuration of its profile was taken in accordance with standard recommendations [13].

The relationship between the flow velocity and the readings of the micromanometer for the Venturi tube corresponds quite accurately to the Bernoulli law in the form

$$v_g = \sqrt{\left(\frac{2\Delta p}{\rho\left(\left(\frac{d_1}{d_2}\right)^4 - 1\right)}\right)},$$

where d_1 is the inside diameter of the tube (21.5 mm) and d_2 is the diameter of the narrowed part of the Bernoulli tube (18.6 mm).

In adjusting the device, the measurement accuracy was checked through the comparison of the readings of the Venturi tube to those of the Prandtl tube. The disagreement did not exceed several percent.

Since the low-temperature channel was open in the upper part for taking air from the atmosphere (Fig. 5), we could measure the flow in this channel using a static-pressure tube. The tube was installed directly into the open part of the porous layer and was calibrated according to the readings of the Venturi tube. Figure 8

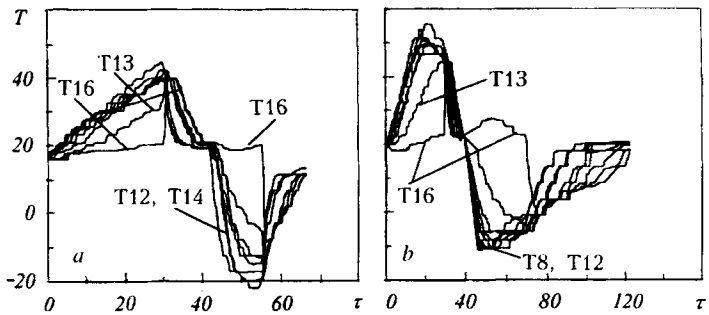

Fig. 9. Thermograms of the thermal effects of phase transition in the thermoreactive medium of the low-temperature channel of a metal-hydride thermal converter. The positions of the thermocouples are the same as in Fig. 6. T, °C; τ, min.

presents a parabolic approximation of the calibration data for checking the possibility of practical calculations of the hydraulic resistance of the layer by the formula [14]

$$\frac{\Delta p}{L} = \frac{150\mu (1-\varepsilon)^2}{\varepsilon^3 d^2} v_g + \frac{1.75\rho (1-\varepsilon)}{\varepsilon^3 d} v_g^2, \tag{7}$$

where L is the length of the static-pressure tube inside the porous medium (0.07 m). Direct recalculation of the data by formula (7) for the air flow at T = 293 K and atmospheric pressure for a monodisperse layer with a particle size of 3 mm and a porosity of 0.4 showed a high convergence of the data of the experiment and calculation on the coefficient on the linear term of Eq. (7). The coefficient on the quadratic term in the experimental evaluation exceeds threefold the theoretical value. This disagreement can, apparently, be assigned to the additional turbulization of the filtered flow on the particles of the porous medium because of their difference in size and the deviation of their shape from a spherical one. This tendency is in qualitative agreement with the theory and experiment [15].

4. Results of the Experimental Investigation. It is convenient to relate the initial concept of the thermal-converting properties of a thermoreactive medium to investigating the *thermal effects of the phase transition in the system of charged thermal converters.* The thermograms of the indicated processes can be seen in Fig. 9a. First the metal-hydride pairs were charged for 40 min under the conditions of absence of filtration of the air flow in both channels. The high-temperature poles were heated up to 200°C. Once the indicated temperature was attained we continued to maintain it at the same level by means of computer control. Then the low-temperature channel was blown through by the air flow at a rate of 1 m/sec for 10 min. The heaters were switched off after the charging. As a result, the high-temperature poles of the charged metal-hydride pairs had a temperature of 200°C while the low-temperature ones were cooled down to the ambient temperature.

In the subsequent sharp cooling of the poles of the high-temperature channel by the air flow at a rate of 1 m/sec, there occurred the opposite redistribution of hydrogen between the poles (discharging of the pairs). The hydrogen was released from the hydride phases of the low-temperature poles. The alloy mass was allowed to cool and cooled the adjacent elements of the pole, the porous medium, and the enclosing structures of the channel. The entire sequence of these events is shown in Fig. 9a. The cooling of the poles of the high-temperature channel for 12 min led to a local generation of cold in the porous medium with a temperature of about −20°C. This corresponds to the permissible thermal limit of the metal-hydride pair whose high-temperature poles are cooled down to 20°C. The calculation by Eqs. (3) for alloys that are characterized by the composition Y = 0 and 0.4 yields a temperature of −22.6°C for the center of the area of the isobar of equilibrium (η = 1/3) with allowance for the equilibrium hysteresis. This effect of cooling is temporary and local in character since, in a rather large time interval, the temperature field in the low-temperature channel levels off and settles at an adiabatic temperature of −4°C. It is precisely this temperature that is recorded as the outlet temperature of a

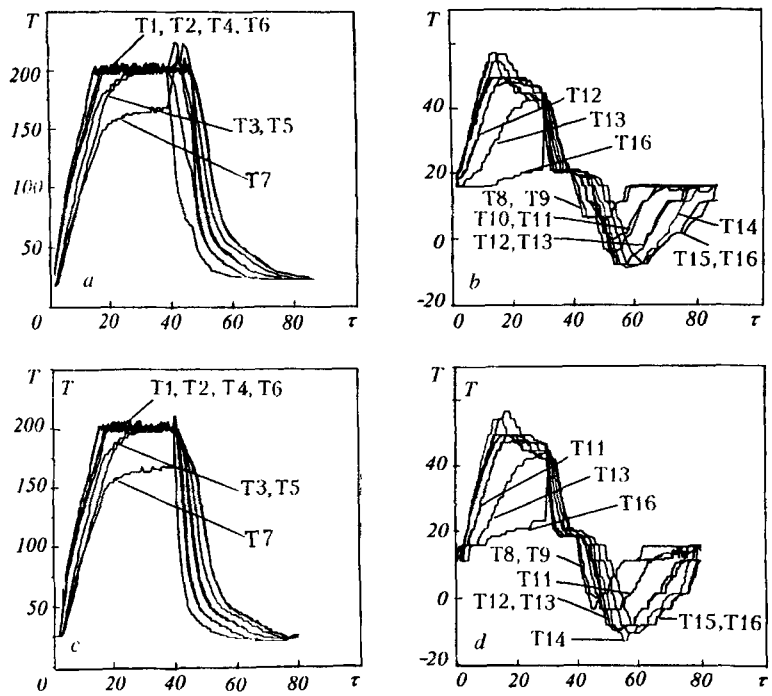

Fig. 10. Thermograms of the development of heat waves in the high-temperature (a, c) and low-temperature (b, d) channels of a thermal converter. The positions of the thermocouples are the same as in Fig. 6.

cold heat wave in the low-temperature channel when the air flow was filtered through it at a rate of 1 m/sec in the final stage of the process. The high-temperature channel was not blown through.

The attainment of lower temperatures in the initial stage of the process is associated with the fact that the adiabatic temperature of cooling of the alloy itself can attain an extremely low mark. Its universal evaluation for arbitrary-type alloys can be related to an enthalpy of the phase transition of about 30 kJ/mol, the mass capacity of the alloy with respect to hydrogen (a hydrogen atom per atom of metal AB_2H_3 or AB_5H_6), and the heat capacity of the alloy evaluated as $3R$ per each metal atom in an alloy molecule:

$$\Delta T_{ad} = \frac{\Delta h}{6R}. \tag{8}$$

The heat capacity of the hydrogen in the composition of the hydride is disregarded.

The thermal effect of the adiabatic reaction that is calculated by formula (8) is equal to 600°C in the indicated parameters. Clearly the thermal limit of the pair is limiting for such a high adiabatic effect.

More real information on the average adiabatic temperature can be provided under the conditions of the experiment whose thermogram is presented in Fig. 9b. Here, a 30-min time delay was performed after cooling the high-temperature channel to redistribute the cold of the phase transition over all the components of the porous medium. The obtained temperature of –4°C reflects the actual adiabatic temperature of the thermoreactive medium in its adopted definition (4).

The data on the *development of heat-energy conversion waves* in the thermoreactive media of a two-channel thermal converter are presented in Fig. 10 a and b.

In the first stage of the experimental investigation, the high-temperature poles were heated under conditions of the absence of air-flow filtration. One can see here temperature troughs in the porous-medium regions, located between the metal-hydride poles (T3, T5, and T7). At the beginning of the filtration (τ = 30 min) the temperatures in these intervals approach the poles' temperatures because of the intense transport of heat with the filtered-air flow. Then, as the heating sources are disconnected (τ = 40 min), one can see the hot

region gradually leaving the porous medium of the high-temperature channel and the heat wave causing progressive cooling of the channel's layers as it moves. During progressive cooling the high-temperature poles become capable of receiving hydrogen from the low-temperature poles paired with them, thus inducing negative heat sources that result from the phase transition inside the low-temperature alloy mass. The thermal effect at the first pole turns out to be minimum since the heat of the phase transition is to a great extent expended on the starting precooling of the elements of the poles and the ambient porous medium. Then the cold generated in the vicinity of the first pole shifts in the form of a heat wave to the neighborhood of the second pole, where the heat wave receives an additional portion of cold from this pole, becomes stronger, and continues its motion to the vicinity of the third pole, where the indicated operational procedure recurs. The intensifying heat wave attains its thermal limit, equaling $-10.7^{\circ}C$, which exceeds the adiabatic temperature of the system. This low temperature level is due to the heating of the flow up to $30^{\circ}C$ as the latter is directed to the high-temperature channel due to the dissipation of energy in a vortex pumping device. It should be noted that the obtained thermal effect of the heat-energy conversion exceeds $40^{\circ}C$.

Thus, the interaction of the poles of the thermal converter through a heat wave makes it possible to overcome the adiabatic limit of the process and contributes to attaining its thermal limit, which was predicted earlier as a result of a simplified analysis in [3, 7, 16]. The process becomes superadiabatic due to the recirculation of heat from pole to pole. The thermal efficiency of this process depends on the relation of the filtration rates of gas flows in the channels of the thermal converter. Indeed, the heat-wave velocity in the high-temperature channel controls the effective motion of the negative heat source in the low-temperature channel, and the air-flow filtration rate in the low-temperature channel determines the transfer of cold in the form of a free heat wave. It is obvious that the greatest thermal effect is attained in a synchronous motion of the cold source and the free heat wave (the condition of thermal resonance).

We can assume that the parameters of the experiment whose thermograms are presented in Fig. 10c and d correspond to the indicated condition. The velocities of the filtered air flows in the high-temperature and low-temperature channels for this experiment equal 0.437 and 0.239 m/sec, respectively.

In the experiment presented in Fig. 10a and b, the velocities of the filtered air flows in the high-temperature and low-temperature channels are 0.437 and 0.310 m/sec, respectively. For this velocity relation, the negative heat source anticipates the free heat wave, which directly leads to the loss of the resulting thermal effect of the process that is expressed in the temperature of the air flow flowing out of the low-temperature channel (T16).

CONCLUSIONS

1. We developed and manufactured an experimental model of a two-channel metal-hydride thermal converter that realizes the process of heat conversion in the regime of a superadiabatic wave of cold.

2. We developed and manufactured an experimental stand that supplies the experimental model with a complete required set of means for measuring and diagnosing the thermal and energy efficiency of the process that realizes a new concept of heat-energy conversion.

3. We revealed experimentally the dynamics of the establishment of the adiabatic temperature in a low-temperature channel that, in the initial stage of the process, manifests itself as adiabatic cooling of the alloy itself with the realization of a local thermal limit and then leads to the establishment of the adiabatic temperature of a thermoreactive porous medium which is represented by its multiple components.

4. We established the effect of the intensification of a heat wave (wave of cold) up to the thermal limit of the hydrogenation reaction that exceeds its adiabatic limit for this thermoreactive medium. The process of propagation of the superadiabatic wave of heat-energy conversion confirms qualitatively the basic results of a theoretical prediction obtained by the methods of numerical modeling.

5. The experimental investigation showed that the earlier mathematical model based on the concept of a quasihomogeneous thermally converting medium reflects only the physical aspect of the process. Numerical modeling of an actual process must allow for both the structural features of built-in poles and the multidimensional configuration of the heat wave that interacts with each individual pole.

This work was carried out under a program of the Fund for Fundamental Research of the Republic of Belarus (grant T97-229).

NOTATION

c, specific heat, J/(kg·deg); d, diameter of the particles of the porous medium; Δh, change in enthalpy when hydrogen changes to the hydride form, J/mol; m, mass, kg; k_{T1} and k_{T2}, coefficients that determine the slope of the areas of the equilibrium isotherms (k_{T1}, in the η range of 0 to 1/3, k_{T2}, of 1/3 to 1); Δm_{H_2}, number of moles of hydrogen involved in the phase transition, mol; n, number of hydrogen atoms per alloy molecule, at/mol; M, hydride-forming alloy; n_{max}, maximum number of hydrogen atoms per alloy molecule; p, hydrogen pressure, Pa; Δp, pressure difference, Pa; Q_L, heat energy of the refrigeration cycle, J; R, universal gas constant, J/(mol·deg); $R_{t\,in}$, internal thermal resistance; $R_{t\,ex}$, external thermal resistance, K/W; ΔS, change in entropy when hydrogen changes to the hydride form, J/(mol·deg); T, temperature, K; T_{ad}, adiabatic temperature of phase transition, K; ΔT_t, thermal limit of heat-energy conversion on the metal-hydride pair, K; $\Delta T_{t\,max}$, equilibrium thermal limit, K; v, velocity, m/sec; W, power of heat-energy conversion, W; Y, stoichiometric constant that determines the alloy composition; η, relative concentration of hydrogen in the hydride ($\eta = n/n_{max}$); ρ, density of the air flow, kg/m^3; μ, dynamic-viscosity factor of air, Pa; ε, porosity; τ, time, min. Subscripts: c, stage of charging of the metal-hydride pair; d, discharging stage; S, sorption; D, desorption; g, gas; h, hydride; H, high-temperature hydride; L, low-temperature hydride; t, thermal; e, equilibrium; 0, ambient medium; p, pole.

REFERENCES

1. F. E. Lynch, *J. Less-Common Metals*, **172-174**, 945-958 (1991).
2. G. A. Fateev and J.-Y. Lee, in: *Collected Papers of the KHES*, Spring Annual Meeting'99, Kwangju, Korea (1999), pp. 27-32.
3. Kyu-jong Kim, *Inzh.-Fiz. Zh.*, **71**, No. 1, 51-61 (1998).
4. T. Domschke, T. Nietsch, and E. Schutt, *Int. J. Hydrogen Energy*, **16**, 255-263 (1991).
5. M. Ron, E. Bershadsky, and Y. Josephy, *J. Less-Common Metals*, **172-174**, 1138-1146 (1991).
6. T. Imoto, T. Yonesaki, S. Fujitani, L. Yonezu, N. Hiro, K. Nasako, and T. Saito, *Int. J. Hydrogen Energy*, **21**, 451-455 (1996).
7. G. A. Fateev and O. S. Rabinovich, *Int. J. Hydrogen Energy*, **22**, 915-924 (1997).
8. J.-Y. Lee and J.-M. Park, *J. Less-Common Metals*, **160**, 259-271 (1990).
9. J.-M. Park and J.-Y. Lee, *Hydrogen Storage Materials of Zr-Ti-Cr-Fe*, US Patent 5028389, Priority data – May 17 (1989).
10. J. H. de Boer, in: *Dynamic Character of Adsoption* [Russian translation], Moscow (1962), p. 215.
11. P. Dantzer and E. Orgaz, *Int. J. Hydrogen Energy*, **11**, 797-806 (1986).
12. G. A. Fateev, K.-J. Jang, J.-G. Park, S.-C. Han, and J.-Y.Lee, in: *Proc. 5th Korea–Japan Joint Symp. '99 on Hydrogen Energy*, Taejon, Korea, November 26, 1999, pp. 61-68.
13. S. M. Gorlin, in: *Experimental Aeromechanics* [in Russian], Moscow (1970), p. 186.
14. M. E. Aérov, O. M. Todes, and D. A. Narinskii, in: *Apparatuses with a Stationary Granular Bed* [in Russian], Leningrad (1979), p. 46.
15. B. M. Galitseiskii and A. L. Lozhkin, in: *Proc. IVth Minsk Int. Forum on Heat and Mass Transfer "Heat and Mass Transfer–MIF-2000,"* Minsk, May 22-26, 2000 [in Russian], Vol. 8. "Heat and Mass Transfer in Capillary-Porous Media," Minsk (2000), pp. 14-23.
16. G. A. Fateev and O. S. Rabinovich, in: *Proc. 27th Int. Symp. on Combustion*, Boulder, Colorado, August 2-7 (1998), pp. 2451-2458.